

Research

Open Access

A nano-view of West Nile virus-induced cellular changes during infection

Jason WM Lee and Mah-Lee Ng*

Address: Department of Microbiology, 5 Science Drive 2, National University of Singapore, Singapore 117597, Singapore

Email: Jason WM Lee - g0300962@nus.edu.sg; Mah-Lee Ng* - micngml@nus.edu.sg

* Corresponding author

Published: 29 June 2004

Received: 05 April 2004

Journal of Nanobiotechnology 2004, 2:6 doi:10.1186/1477-3155-2-6

Accepted: 29 June 2004

This article is available from: <http://www.jnanobiotechnology.com/content/2/1/6>

© 2004 Lee and Ng; licensee BioMed Central Ltd. This is an Open Access article: verbatim copying and redistribution of this article are permitted in all media for any purpose, provided this notice is preserved along with the article's original URL.

Abstract

Background: Microscopic imaging of viruses and their interactions with and effects on host cells are frequently held back by limitations of the microscope's resolution or the invasive nature of the sample preparation procedures. It is also difficult to have a technique that would allow simultaneous imaging of both surface and sub-surface on the same cell. This has hampered endeavours to elucidate virus-host interactions. Atomic Force Microscopy (AFM), which is commonly used in the physical sciences, is now becoming a good correlative form of microscopy used to complement existing optical, confocal and electron microscopy for biological applications

Results: In this study, the West Nile (Sarafen) virus-infected Vero cell model was used. The atomic force microscope was found to be useful in producing high resolution images of virus-host events with minimal sample processing requirements. The AFM was able to image the budding of the West Nile (Sarafen) virus at the infected cell surface. Proliferation of the filopodia and thickening of clusters of actin filaments accompanied West Nile virus replication.

Conclusions: The study shows that the AFM is useful for virus-host interaction studies. The technique provides morphological information on both the virus and the host cell during the infection stages.

Background

Viral infections represent a particularly difficult type of challenge to overcome. Though the field of anti-viral strategies continues to grow, success rates lag greatly behind antibacterial strategies. This is due in large part to the lack of understanding of virus interactions with their host cells. The small scale of viruses results in difficulties in the efficient imaging of virus-infected samples.

To date, the microscopy forms that are able to achieve the level of magnification and resolution for imaging viruses are the scanning electron microscope (SEM) and transmission electron microscope (TEM). Both these techniques have a requirement for tedious levels of sample process-

ing. The invention of the atomic force microscope (AFM) by Binnig and colleagues [1] has allowed for high-resolution imaging of nanostructures in living samples [2-4]. A number of these studies involved the observation of purified samples of biomolecules including large viruses, for example, the tobacco mosaic virus, pox virus and human immunodeficiency virus [5-7]. The homogeneity in the sample appears to lend itself to better AFM imaging.

The AFM is able to produce images in several different formats, of which three were consistently analysed: height, phase and amplitude. The height data image is obtained via recording the changes in AFM scanner height as it shifts to keep the vibrational amplitude of the cantilever

of the probe constant. This produces an image with highly accurate quantitative height measurements. The phase data image produces an image that provides information of the differing materials/texture in the sample by analyzing the different responses of the probe on such materials. The amplitude data image produces an emphasized view of the height data image by describing the change in the amplitude of the probe directly. While structures are not distorted in the amplitude data image, accurate quantitative measurements are more likely garnered from the height data image.

The AFM does not require much in sample processing: in fact, its main requirement is that the sample is well-adhered to a substrate such that it does not move around when the AFM probe engages it. Beyond that, additional sample preparation such as fixation or labelling is decided on a sample-specific basis. While a live sample would be an ideal specimen to study, biosafety concerns stipulated the use of mild fixation in our virus infected samples. Fixation was preformed on mock-infected samples for the sake of consistency. As a result, the observations in the study are based on the interpretation of static pictures.

The objectives of this study are to investigate the suitability of atomic force microscopy for virus-host interaction studies using the flavivirus model. In addition, to gauge if the images obtained can reveal more information than with the known conventional ultra-structural studies.

Results and Discussion

West Nile (Sarafend) virus-induced changes in infected cells at late stage infection

At the late stages of West Nile (Sarafend) virus infection in Vero cells, several interesting aspects warranted investigation. One unique aspect was the maturation of this virus at the plasma membrane. This observation was first reported by Ng and colleagues [8,9]. Active budding was also present at the proliferated filopodia. In conjunction with the budding of the maturing virus particles, there was a progressive lengthening and thickening of the actin filaments at the cell peripheral. The postulation was that the vectorial force of the growing length of the actin filament provided the bending force to expel the virus particles [10].

Figs. 1a & 1b show a budding virus (arrowhead) extruding from the plasma membrane at 24 h p.i. Fig. 1b shows a higher resolution scan of the extruding virion, with the envelope clearly surrounding the virus nucleocapsid (arrowhead). A TEM image of a virus particle (Fig. 1c) was included for comparison. The arrowheads point to the extruding progeny virions while the arrow indicates the electron dense immunogold label targeted against the

WNV envelope protein. The AFM image gave a 3-dimensional view of the entire budding virus.

The hard tapping AFM technique used provided a certain degree of "translucency" to the plasma membrane, which enabled the imaging of sub-surface structures in addition to producing surface morphological data. By adjusting the probe to engage the sample with greater force, the probe tip physically pushes against the soft sample surface to image sub-surface structures. It was through this ability that the AFM was able to observe the up-regulation of actin filaments in the late infection stages.

In Fig. 2 the formation of actin filaments near the cell periphery in infected cells was seen over time. Fig. 2a shows some degree of enhancement of the cytoskeleton network around the cell periphery (arrow) in the West Nile (Sarafend) virus-infected Vero cells at 12 h p.i. Fig. 2b shows an increased degree of cytoskeletal thickening (arrow) of similarly infected cells at 16 h p.i. It is noted that the formation of cytoskeleton clustering in the infected cells appears to be proximal to the formation of filopodia. The three-dimensional reconstruction of Fig. 2b illustrates the induced skeletal filaments (Fig. 2c, arrows) encroaching into newly formed filopodia (arrowheads). This detailed progression of cytoskeleton enhancement cannot be visualized by the SEM (as it can only provide surface morphology data) or TEM (as it can only provide 2-dimensional data). A lower magnification scan of a mock-infected Vero control cell is provided in Fig. 2d. While the endoplasmic reticulum region is clearly observed at the perinuclear region (arrow), there is the lack of the filopodia and cytoskeleton clustering that is observed in the West Nile virus-infected cells at the periphery of the plasma membrane.

At late infection, filopodia were readily seen to be radiating from the infected cell periphery. These structures were not seen in mock-infected Vero cells at 36 h p.i. (Fig. 3a). These control cells also showed a lack of cytoskeletal formation at the periphery of the plasma membrane when compared to infected cells. Fig. 3b shows the filopodia (arrows) formation between four infected host cells at 36 h p.i. Fig. 3c shows bags of virus particles (thin arrows) liberated from the cells surface as well as the filopodia at 36 h p.i. During this stage of infection when the cytopathic effects were advanced, progeny viruses no longer budded out individually but in bags [9]. The thick arrow shows regions of cytoskeleton thickening in the infected cells. Arrowhead points to the virus-induced filopodia formation. The TEM micrograph in Fig. 3d confirmed similar bags of virus particles (arrows) at the extracellular space. Arrowhead shows the filopodia, but these were not as pronounced as in the AFM imaging due to required ultrathin sectioning of the sample.

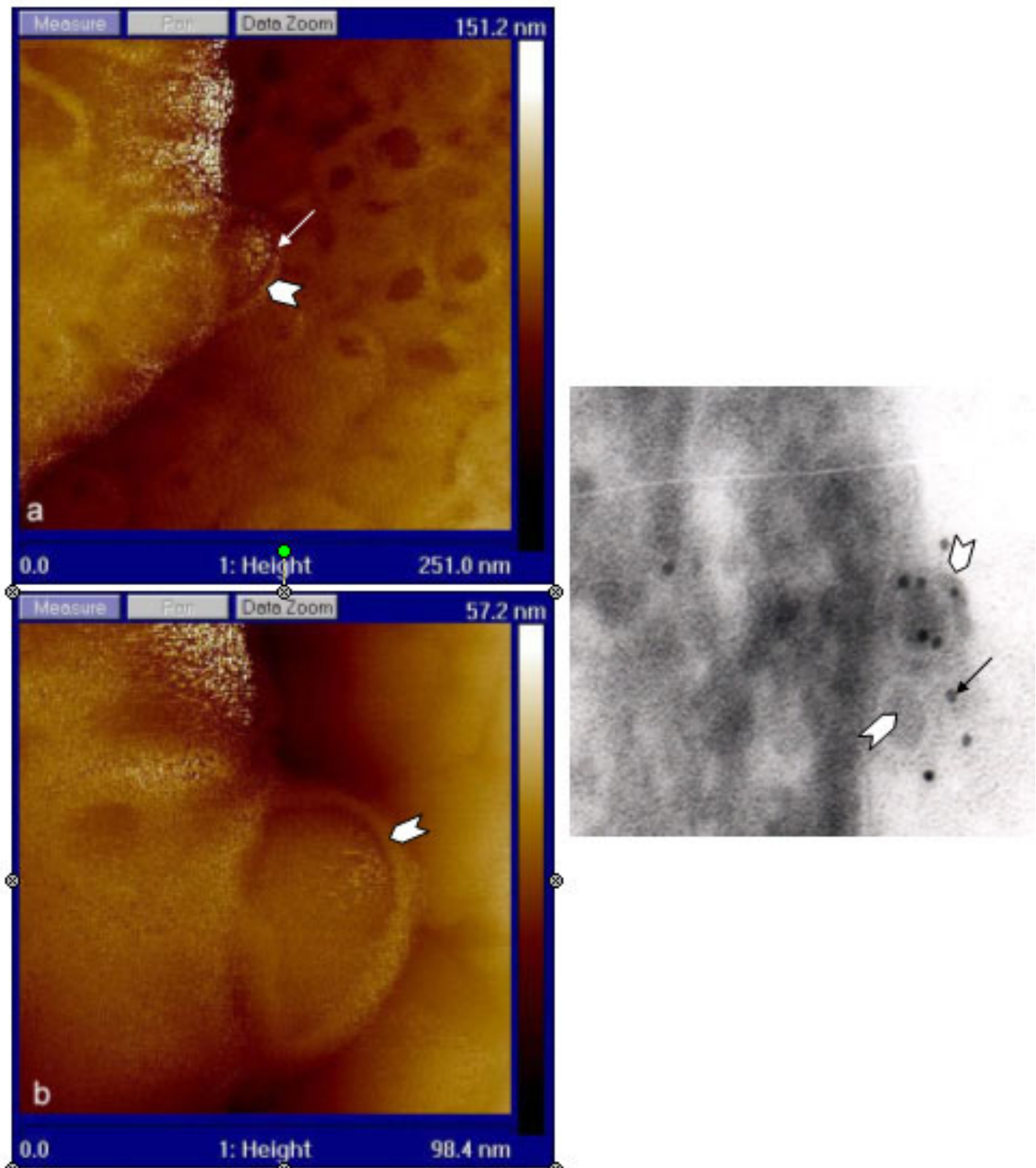


Figure 1

(a) AFM height scan of West Nile virus-infected Vero cells at 24 h p.i. Scan size is 251 nm × 251 nm. A progeny virus (arrow) budding from the plasma membrane of the host cell. (b) AFM height scan of West Nile virus-infected Vero cells at 24 h p.i. Scan size is 98.4 nm × 98.4 nm. Arrowhead shows the envelope surrounding the budding progeny virus. (c) TEM image of West Nile virus-infected Vero cells (arrowheads) budding from host cell. The electron dense dots are the immunogold particles targeted against the envelope protein of the WNV.

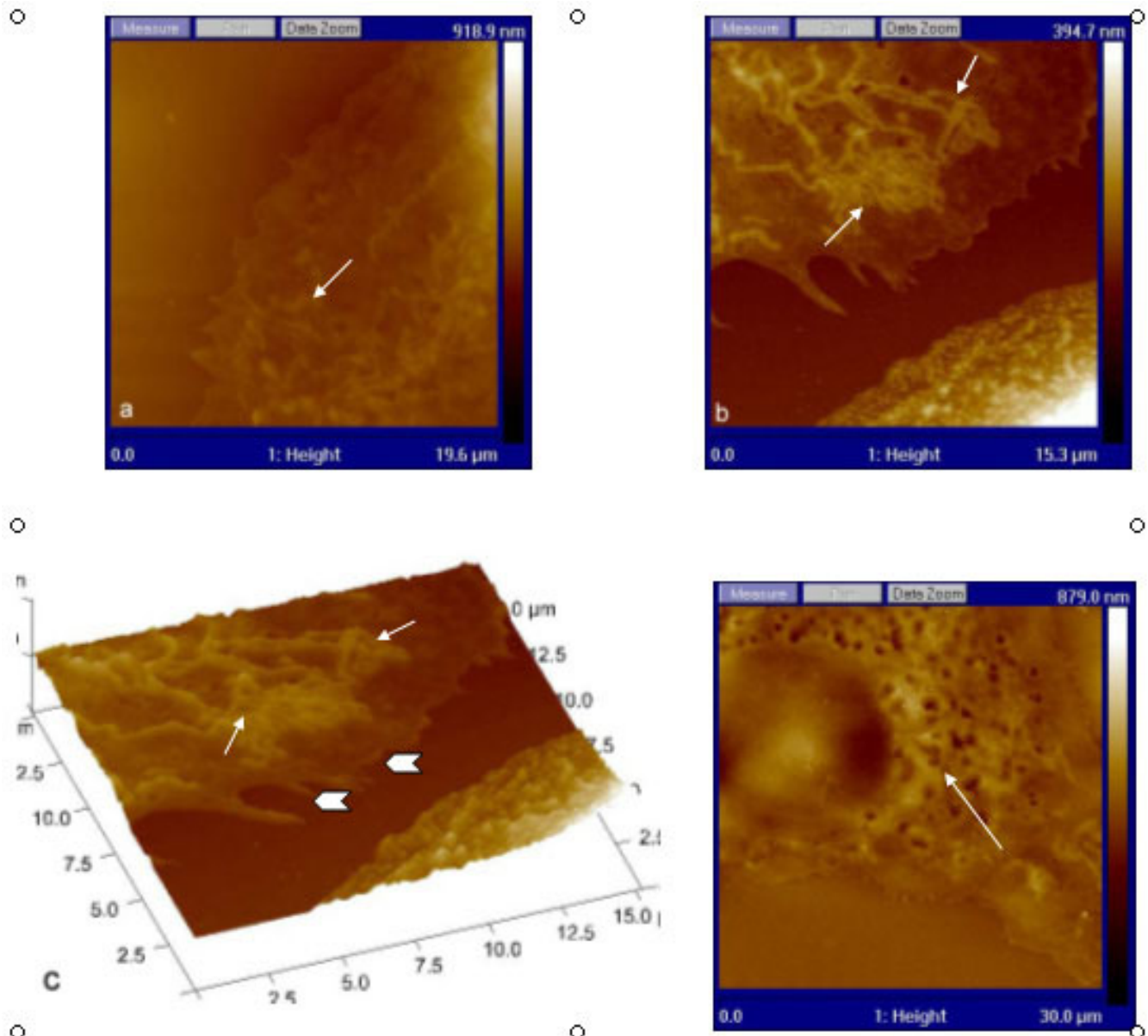


Figure 2

(a) AFM height scan of West Nile virus – infected Vero cells at 12 h p.i. Scan size is $19.6 \mu\text{m} \times 19.6 \mu\text{m}$. Arrow shows some degree of enhanced cytoskeleton formation. (b) AFM height scan of West Nile virus – infected Vero cells at 24 h p.i. Scan size is $15.3 \mu\text{m} \times 15.3 \mu\text{m}$. Arrows show greater degree of thickening and clumping of actin filaments in close proximity to the cell periphery of the infected cell at 16 h p.i. (c) AFM 3D height scan of $15.3 \mu\text{m} \times 15.3 \mu\text{m}$ size. Arrows show the actin filaments forming near the cell edge and the nascent filopodia (arrowheads). (d) AFM height scan of mock-infected Vero cells at 24 h p.i. Scan size is $30 \mu\text{m} \times 30 \mu\text{m}$. This control cell shows a lack of cytoskeleton thickening and clumping at the periphery of the cell plasma membrane. The rough endoplasmic reticulum is indicated by the arrow.

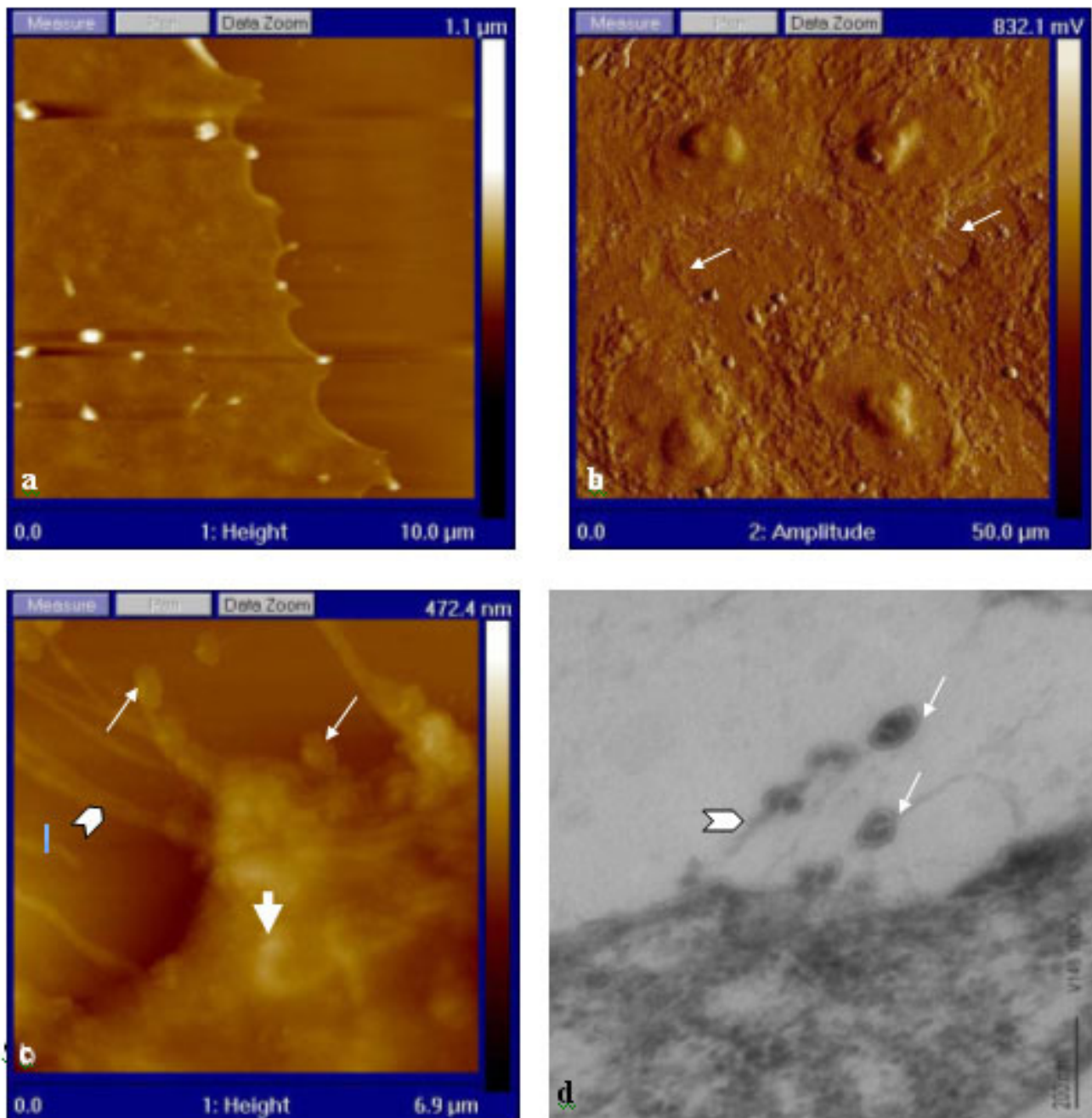


Figure 3

(a) AFM height scan of mock – infected Vero cells at 36 h p.i. Scan size is 10 μm × 10 μm. In the mock-infected control sample, a distinct lack of filopodia and cytoskeleton formation is obvious. The bright spots depict high regions of the cells. (b) AFM amplitude scan of West Nile virus – infected Vero cells at 36 h p.i. Scan size is 50 μm × 50 μm. Arrows show the filopodia produced by these four infected cells. (c) AFM height scan of West Nile virus – infected Vero cells at 36 h p.i. of 6.9 μm × 6.9 μm size. Thin arrows show enveloped bags containing progeny West Nile viruses as they egress from host Vero cells. The arrowhead shows the filopodia formed in infected cells. Thick arrow shows the actin filaments near the budding enveloped bags. (d) The transmission electron micrograph shows similar image as in (c). The bags of virus (arrows) are seen exiting from the cell filopodia (filopodia).

Conclusions

The AFM successfully imaged the West Nile virus-induced changes in infected Vero cells. Both the TappingMode™ and hard tapping mode were used in this study. As this is the first study using atomic force microscopy for flaviviruses, a more cautious approach was taken. Mildly-fixed infected cells were used to optimize the AFM technique for virus-host interaction studies. To gain further confidence with this technique, transmission electron micrographs were included for comparison. As these samples were fixed and dried prior to imaging, certain considerations had to be addressed.

The effects of this drying procedure may cause a certain degree of flattening to the nanostructures on the sample, and this was taken into account during interpretation of the results. Drying may also increase the surface roughness [11] of the sample. However, the effect of fixation on these samples brings the samples morphologically more similar to the TEM images that we used for comparison, and made such comparisons more meaningful. At such an early stage of research, confirmations and corroboration from other more established microscopy forms are essential to successfully interpret the results from the AFM.

Since the cells are soft textured samples, TappingMode™ was the preferred mode used. The alternative contact mode involves the constant contact between the probe and the sample, thus causing damage to the soft biological samples. Hard tapping was applied when there was a need to image sub-surface structures. These modes proved to be very compatible for virus and cell imaging.

In the case of West Nile (Sarafend) virus infections, the new information provided by the AFM gave further insight into virus-induced changes during the infection. Nanostructures such as the budding of individual progeny viruses (Fig.1) or of bags containing progeny virus were observed as enveloped sacs associated with the filopodia extending from the plasma membrane in the West Nile virus-infected Vero cells (Fig. 2). The AFM can image the virus-induced changes in the host cell as well as minute structures (50 nm) such as West Nile virus particles illustrates that the AFM is able to provide both the macro and nano data germane to virus-host interaction studies. The usefulness of hard tapping techniques was most notable in the observation of actin filament formation near the periphery of the infected cell membrane. The time course of West Nile virus infection through the Vero cell has been documented in previous studies [8-10] using other microscopy forms, and they corroborate the observations made in this study using the AFM.

The virus studied here is of great medical and economical impact on the world. Flaviviruses have long been a medi-

cal problem in many parts of the world [12], especially with the resurgence of West Nile virus infections in North America [13]. With emerging and re-emerging viruses such as this, new and pertinent data of how these viruses replicate in their host cells is becoming increasingly and urgently needed. The nano-biotechnological field of AFM represents a new set of "eyes" in which virologists may use to meet these new challenges.

Methods

Cells

Vero cells derived from African green monkey kidney (a kind gift from Professor E. G. Westaway, Sir Albert Sakzewski Virus Research Laboratory, Queensland, Australia) were used. Cell lines were maintained in M199 growth media supplemented with 10% foetal calf serum (FCS). Cells were cultured onto sterile ethanol-treated coverslips placed into 24-well cell culture plates and incubated overnight to achieve a level of 80% confluency. These cells were used for virus infection studies.

Virus

West Nile (Sarafend) virus, a kind gift from Professor E. G. Westaway, Sir Albert Sakzewski Virus Research Laboratory, Queensland, Australia), was propagated in Vero cells throughout this study.

Flavivirus infection of cells

The Vero cells were infected with West Nile (Sarafend) virus at a multiplicity of infection (M.O.I.) = 1. The cells grown on the coverslips were washed once with PBS, before infection with 100 µl of viruses for 1 h. The coverslips were rocked gently every 15 min to ensure the uniform spreading of the virus solution over the cell monolayer on the coverslip. After 1 h of infection, 1.5 ml of the appropriate growth media supplemented with 2% FCS was added to the coverslips, and these were left to incubate in a 5% CO₂ incubator at 37 °C. The samples were fixed, and imaged at 12, 16, 24 and 36 h p.i.

Sample preparation

As this is a pioneering study on the flavivirus, mildly fixed samples were used. The samples were washed thrice with PBS for the duration of 5 min each time, after which they were fixed with a 2% paraformaldehyde/0.2% glutaraldehyde solution at pH 7.4 for 30 min. The fixative solution was decanted and the samples washed twice with PBS. A final wash with deionised water was followed by gentle drying with a nitrogen gas gun.

AFM

The samples were then imaged in the AFM using the Force Modulation Etched Silicon Probe (FESP), (Veeco, USA) which has a length of 219 µm and a vibrational frequency of 69-88 kHz.

Cryo-Immunolabelling Electron Microscopy

At selected times p.i., Vero cells infected with WNV were washed twice with cold PBS and fixed with 0.2% glutaraldehyde/ 4 % paraformaldehyde for 30 min. The cells were scraped and spun down. The cell pellet was resuspended in 10% gelatin at room temperature and spin, and the gelatin with the pelleted cells was solidified at 4°C for 10 min. The hardened block was post-fixed with the above fixative again for 20 min. The gelatin block was then cut into 1-mm cubes and immersed into cryo-protection buffer of 2.3 M sucrose for 2 h. The block was frozen by plunging into liquid nitrogen before cryo-ultramicrotomy, using an ultracut microtome (UCT) with a cryo-attachment (EM FCS – Leica, Austria). Ultrathin sections of the infected cells were picked up onto Formvar-coated grids and immunolabelling was carried out at room temperature. The sections were washed for 10 min with PBS. This was followed by three washes (at 5 min each) with 0.05 M glycine in PBS (to block the aldehyde groups) before incubating for 30 min in PBS with 5% BSA (protein block). Sections were then washed in 0.1% BSA in PBS (3 × 5 min) and exposed to the primary antibody (against the WNV envelope protein) at 1:100 dilution (0.1% BSA in PBS) for 1 h. Six washes (at 5 min each) in 1% BSA in PBS was done before exposing the cells to the Protein A colloidal gold (10 nm at 1:20 dilution to label envelope protein) for 1 h. Samples were then postfixed in 2% glutaraldehyde in PBS for 5 min and washed (2 × 5 min) in PBS and distilled water (4 × 5 min). Finally, sections were embedded in 2% uranyl acetate and 1.8% methyl cellulose mixture (1:9 parts) for 5 min and dried before viewing under the CM120 BioTwin transmission electron microscope (Philips, The Netherlands).

List of Abbreviations Used

AFM: Atomic Force Microscope

TEM: Transmission Electron Microscope

SEM: Scanning Electron Microscope

LM: Light Microscope

PBS: Phosphate Buffered Saline

BSA: Bovine Serum Albumin

h p.i.: hours post infection

Authors Contributions

JL carried out the sample preparation and AFM studies. NML conceived of the study, and participated in its design and coordination. Both authors read and approved the final manuscript.

Acknowledgement

This work was supported by the Academic Research Fund (Grant no. R-182-000-055-112), from the National University of Singapore

References

1. Binnig G, Rohrer H: **The Scanning Tunneling Microscope**. *Sci Amer* 1985, **253**:50-56.
2. Allen MJ, Balooch M, Subbiah S, Tench RJ, Siekhaus W, Balhorn R: **Scanning tunneling microscope images of adenine and thymine at atomic resolution**. *Scanning Microsc* 1991, **5**:625-630.
3. Almqvist N, Backman L, Fredriksson S: **Imaging human erythrocyte spectrin with atomic force microscopy**. *Micron* 1994, **25**:227-232.
4. Bai C, Zhang P, Fang Y, Cao E, Wang C: **Studies of biomaterials using atomic force microscopy**. *J Korean Physical Society (Proc Suppl)* 1997, **31**:S47-S50.
5. Drygin YF, Bordunova OA, Gallyamov MO, Yaminsky IV: **Atomic force microscopy examination of tobacco mosaic virus and virion RNA**. *FEBS Lett* 1998, **425**:217-221.
6. Ohnesorge FM, Horber JK, Haberle W, Czerny CP, Smith DP, Binnig G: **AFM review study on pox viruses and living cells**. *Biophys J* 1997, **73**:2183-2194.
7. Kuznetsov YG, Victoria JG, Robinson WE Jr, McPherson A: **Atomic force microscopy investigation of human immunodeficiency virus (HIV) and HIV-infected lymphocytes**. *J Virol* 2003, **77**:11896-11909.
8. Ng ML, Howe J, Sreenivasan V, Mulders JJ: **Flavivirus West Nile (Sarafend) egress at the plasma membrane**. *Arch Virol* 1994, **137**:303-313.
9. Ng ML, Tan SH, Chu JJ: **Transport and budding at two distinct sites of visible nucleocapsids of West Nile (Sarafend) virus**. *J Med Virol* 2001, **65**:758-764.
10. Chu JJ, Choo BG, Lee JWM, Ng ML: **Actin filaments participate in West Nile (Sarafend) virus maturation process**. *J Med Virol* 2003, **71**:463-472.
11. Yu M, Ivanisevic A: **Encapsulated cells: an atomic force microscopy study**. *Biomaterials* 2004, **25**:3655-3662.
12. Westaway EG, Brinton MA, Gaidamovich SY, Horzinek MC, Igarashi A, Kaariainen L, Lvov DK, Porterfield JS, Russell PK, Trent DW: **Flaviviridae**. *Intervirology* 1985, **24**:183-192.
13. Centers for Disease Control and Prevention (CDC): **Update: West Nile-like viral encephalitis, New York, 1999**. *MMWR Morb Mortal Wkly Rep* 1999, **48**:890-892.

Publish with **BioMed Central** and every scientist can read your work free of charge

"BioMed Central will be the most significant development for disseminating the results of biomedical research in our lifetime."

Sir Paul Nurse, Cancer Research UK

Your research papers will be:

- available free of charge to the entire biomedical community
- peer reviewed and published immediately upon acceptance
- cited in PubMed and archived on PubMed Central
- yours — you keep the copyright

Submit your manuscript here:
http://www.biomedcentral.com/info/publishing_adv.asp

